MICROSTRUCTURE AND ELECTROCONDUCTIVITY OF TiN-Al_2O_3 COMPOSITES PREPARED BY HOT-PRESSING

Zhi-Hua Yang[1*], De-Chang Jia[1], Fang Luo[1], Xiao-Ming Duan[2,1], Yu Zhou[1]

[1]*Institute for Advanced Ceramics, Harbin Institute of Technology, Harbin 150001, China*
[2]*National Key Laboratory for Precision Hot Processing of Metals, Harbin Institute of Technology, Harbin 150001, China*

Keywords: Electrical properties, TiN, SiC, hot pressing.

Abstract

After the addition of TiN into Al_2O_3 ceramic, the intensity, toughness and wear-resisting property of the ceramics increased, and the most important thing were the improvement of the electrical property. In this thesis, Al_2O_3-TiN composites were prepared by hot-pressing (HP) technique. And the SiO_2 was added as sintering additives. The TiN powders homogenously distributed in the Al_2O_3 matrix. The ceramics have high mechanical properties: Vickers hardness could attain to 20GPa, and the highest was 25.5 GPa; fracture toughness was between 4 and 6 $MPa{\cdot}m^{1/2}$, and flexural strength could reach 578 MPa. Electrical conductibility tests indicate that the electrical resistivity of TiN-Al_2O_3 ceramics descended with the increasing content of TiN from 5 to 20 vol.%, and the electrical resistivity were between $10^{12}\Omega{\cdot}cm$ to 10^4 $\Omega{\cdot}cm$. The highest on-load voltage of the ceramics could reach 5000 V, meanwhile the current was only 89 nA.

1 Introduction

The multi-gap resistive plate chamber (MRPC) has good time resolution (less than 100 ps) and high detection efficiency (higher than 95%). This technology has been adopted to construct the full barrel time-of-flight (TOF) detector for the STAR experiment at RHIC [1-3]. The cylindrical TOF detector covers a total area of approximately $64m^2$. The whole TOF system consists of 120 trays and each tray consists of 32 MRPC modules. Another six stray are produced as standbys. Thus the total number of modulus is 4032. The structure of MRPC modulus for STAR is shown in Fig. 1 [1]. Each modulus consists of six read-out pads. The size of each pad is 3.15×6.3 cm^2. There is a 3-mm gap between each pad. An MRPC is basically a stack of resistive plates with a series of uniform gas gaps. Electrodes are applied to outer surface of the two outmost plates. A strong electric field is generated in each sub-gap by applying a high voltage (HV) across the external electrodes. All the internal plates are electrically floating. A charged particle going through the chamber generates avalanches in the gas gaps. Because the glass plates are highly resistive, they are transparent to fast charge induction from avalanches in the gaps. Typical resistivity for the glass plates is in the order of about $10^{12}\Omega{\cdot}cm$ [1]. The induced signal on the pads is the sum of possible avalanches from all gas gaps. The electrodes are made of resistive graphite tape and are also transparent to induced signal charge. In present case, the inner glass plates are 0.54mm thick and are kept parallel by using 0.22 mm diameter nylon fishing lines as spacer. The outer glass plates are 0.77 mm thick, and the carbon tape is on the outer glass sheet. The signals are read out by an array of copper pickup pads. The TOF system require the glass plates not only the special resistivity but also have low electric current.

Alumina (Al_2O_3)-based ceramics have been extensively studied because of their excellent properties such as high hardness, low electrical conductivity, good chemical stability and oxidation resistance [4]. Titanium nitride (TiN) has a high melting temperature (2950°C), good electroconductivity and high resistance to corrosion and oxidation [5]. Al_2O_3-based ceramics was reported to increase some mechanical properties, and to lower the electrical resistivity because of the addition of TiN [6-9]. Electroconductive Al_2O_3-based ceramics could be shaped by electrical discharge machining to manufacture complex components. Depending on the amount of TiN particles added and on the type of TiN sub-network formed in the ceramics, electrical resistances was between 10^{14} and 10^{-3} Ω·cm. So we can attain the TiN-Al_2O_3 ceramics with resistivity in the order of about 10^{12} Ω·cm. Besides this, TiN-Al_2O_3 ceramics should have higher strength and lower electric current than glass.

In the present work, dense TiN-Al_2O_3 ceramics with 0-20 vol.% TiN were fabricated by hot-pressed. The mechanical properties and electrical conductivity of the sintered bodies were evaluated.

2. Experimental procedures

Appropriate amounts of α-Al_2O_3 and TiN powders, with average particle sizes of 7.5 μm and 40 nm, respectively, were mixed and milled in absolute ethyl alcohol for 24 hours, to yield a series of Al_2O_3-TiN mixtures with TiN vol.% of 0, 5, 10, 15 and 20. In order to decrease the sintering temperature, 2 vol.% SiO_2 was added as sintering additive. The dried powder mixtures were hot-pressed in a graphite die coated with h-BN at 1600°C for 15 min under a pressure of 25 MPa in vacuum.

The density of the sintered samples was measured using the Archimedes method. The resulting sample ceramics were cut into bars of 36 mm × 3 mm × 4 mm (30 mm outer span) for measuring flexural strength with a crosshead speed of 0.5 mm/min. The fracture toughness was determined using the single edge notched beam method with a crosshead speed of 0.05 mm/min. The testing bar dimensions used were 2 mm × 4 mm × 20 mm (16 mm outer span). The depth of the notches was 2.0 mm and the width about 0.2 mm. The resistivity of sintered bodies was measured by the four-probe method.

The structural characterization of ceramics was analyzed using X-ray diffraction (XRD) methods with CuKα radiation. The investigation of microstructure was done in scanning electron microscope (SEM) and transmission electron microscope (TEM).

3. Results and discussion

3.1 Densification and microstructure of TiN-Al_2O_3 ceramics

The hot-pressed TiN-Al_2O_3 ceramics were almost fully dense, with the densification degree in the range of 98.5-99.9% of the theoretical density (As shown in Table 1). The addition of nano-sized TiN decreased the densification rate of the ceramics. In our experiment, SiO_2 was added into ceramics as sintering additives. And the ceramics, which were hot-pressed at 1600°C for 15 min under a pressure of 25MPa, can get high relative densities. But for the TiN-Al_2O_3 ceramics were also hot-pressed without sintering additives, the same relative densities could be get only when the ceramics sintered at 1650~1750 °C for 45 min under a pressure of 26 MPa [6].

Fig. 1 is the X-ray diffraction pattern of TiN-Al_2O_3 ceramic with TiN content of 10 vol.%. XRD result reveals that the ceramics is composites of c-TiN and α-Al_2O_3. The result indicates that no chemical reaction occurs between them.

Fig. 2 shows the back-scattered SEM micrograph of the polished surface of TiN-Al_2O_3 ceramics. Black particles are Al_2O_3, while white TiN particles located among Al_2O_3 grains.

TiN grains were uniformly dispersed in Al_2O_3 matrix. Fig. 3 shows the microstructure of the fracture cross-sections of TiN-Al_2O_3 ceramics with different TiN contents. It can be seen that the fracture morphology and grain size were significantly influenced by the TiN content in those ceramics. The fracture mode of TiN-Al_2O_3 ceramic with 0 vol.%, 5 vol.% and 10 vol.% TiN was mainly intergranular (as shown by Fig. a), b) and c)). With the increase of the TiN content, facture mode changed. For the ceramics containing 15 vol.% and 20 vol.%, the fracture modes were intergranular and transgranular (as shown by Fig. d) and e)). Those changes of fracture mode were attributed to the grain boundaries were strengthened, inhibiting intergranular crack propagation.

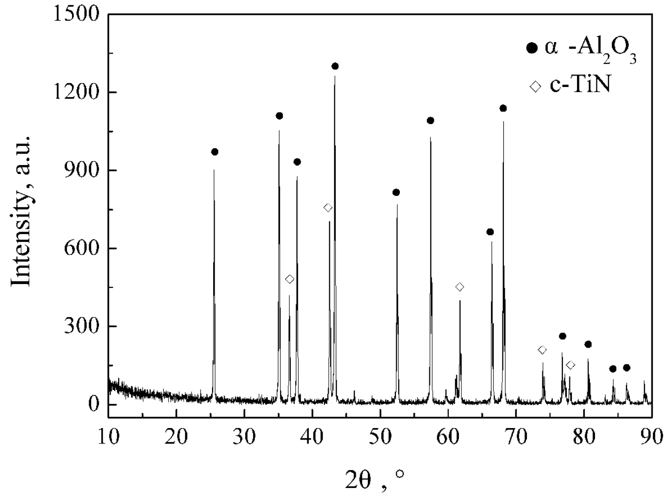

Figure 1. XRD pattern of the hot-pressed Al_2O_3-TiN composites with 10 vol.% TiN

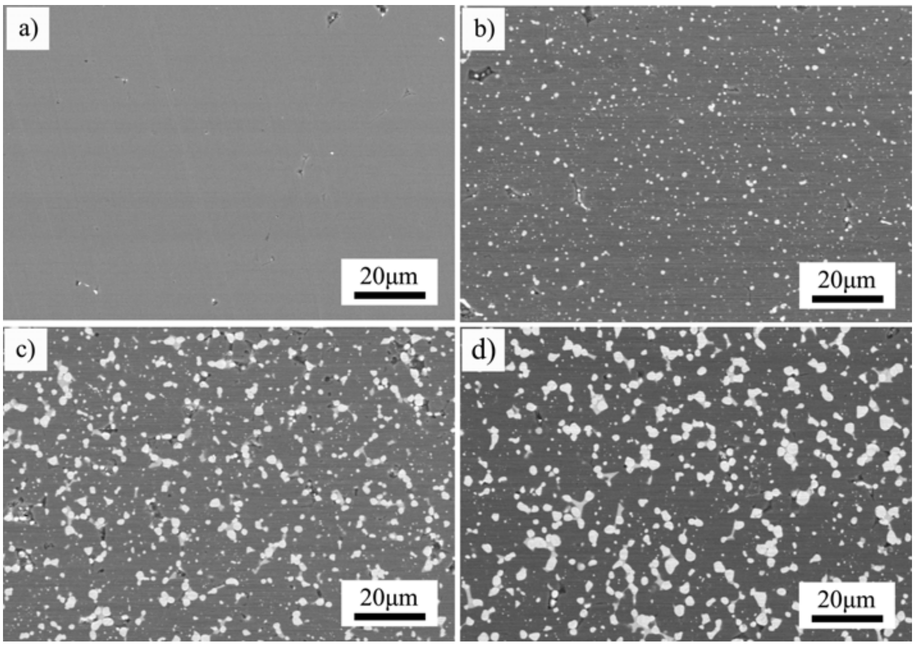

Figure 2. Back-scattered SEM micrograph of polished surface of the hot-pressed Al_2O_3-TiN composites with different content of TiN. a) 0%, b) 5%, c) 15%, d) 20%

3.2 Mechanical properties

Mechanical properties of the TiN-Al_2O_3 ceramics are summarized in Table 1. The flexural strengths of hot-pressed TiN-Al_2O_3 ceramics with various TiN contents from 5 to 25 vol.%

was higher than that of monolithic Al_2O_3 ceramics and the highest flexural strength (578.2 MPa) was achieved at 15 vol.% TiN. The addition of nano-sized TiN particles improves the microstructure and strengthens grain boundaries, which lead to increase in the flexural strengths of the TiN-Al_2O_3 ceramics.

The fracture toughness of TiN-Al_2O_3 ceramics had the same variation trend with the flexural strengths. The highest fractural toughness was 6.02 $MPa \cdot m^{1/2}$. For the TiN-Al_2O_3 ceramics, many toughening mechanism may attribute to explain the increase of the fracture toughness, such as crack pinning, crack bridging, and crack deflection, et al. The crack deflection is very evident, as shown in Fig. 3. In both tested ceramics, with the content of 0 and 15 vol.% TiN, the crack was propagated almost straight from the indentation corner. A slight deflection is connected with the intergranular nature of crack propagation. It is clearly shown that the fine TiN particles did not form a strong barrier for the cracks. The other two possible toughening mechanisms may be crack pinning and crack bridging. Because of the similar thermal expansion coefficient between the Al_2O_3 and TiN, residual stresses and microcracks can be excluded.

Composite (Vol.% TiN)	**Relative density /%**	**flexural strenghs /MPa**	**Fracture toughness /$MPa \cdot m^{1/2}$**	**Elastic modulus /GPa**	**Vicker\`s hardness /GPa**	**Electrical resistivity /$\Omega \cdot cm$**
0	99.9	349.3±9.3	4.18±0.26	388.1±17.4	20.7±1.7	1.78×10^{13}
5	99.4	421.7±11.6	4.68±0.47	414.6±8.2	22.1±2.0	1.17×10^{11}
10	98.8	560.8±15.4	4.42±0.23	416.5±9.1	22.3±2.0	3.88×10^{9}
15	98.2	578.2±10.6	6.02±0.43	430.9±8.7	25.5±1.5	2.42×10^{6}
20	98.5	556.3±9.6	5.06±0.10	443.4±8.1	23.0±2.5	1.52×10^{5}

Table 1. Properties of the hot-pressed TiN-Al_2O_3 ceramics

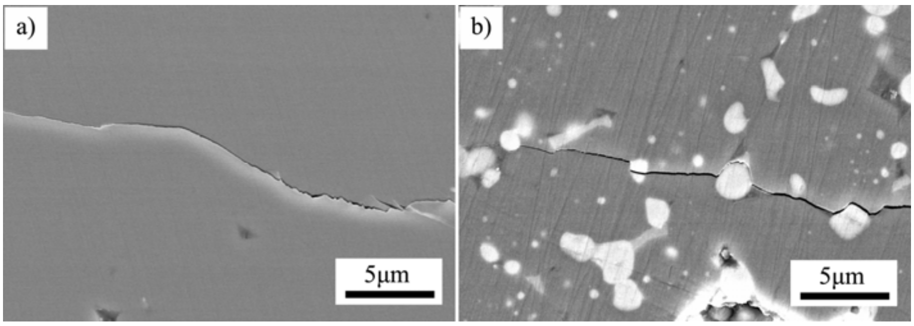

Figure 3. Crack propagation in the ceramics with a) 0 vol.% and b) 15 vol.% TiN nanoparticles

The elastic modulus values increased with the increase of TiN content, from 388.1 GPa for the matrix to 443.4 GPa for the composite with 20 vol.% TiN. The Vicker's hardness of TiN-Al_2O_3 ceramics reaches to a hardness of 25.5 GPa, which was almost the same for different TiN contents from 5 to 20 vol.% and no significant increase from that of monolithic Al_2O_3 ceramics.

3.3 Electrical conductivity

TiN phase is electrical conductive, but the electrical conductivity of Al_2O_3 phase is very low. So the determining factors of electrical conductivity for the TiN-Al_2O_3 ceramics are the content and distribution of the TiN phase. With the increase of TiN content, a network of TiN phase within the Al_2O_3 matrix formed. This phenomenon was can be observed from the back-scattered SEM micrograph (as shown in Fig. 4). The electrical resistivity of TiN-Al_2O_3 ceramics decreased with increasing amount of TiN phase and reach to a minimum value of 1.52×10^5 $\Omega \cdot cm$ for the ceramic with 20 vol.% TiN. So we can see that for the multi-gap resistive plate chamber, the optimum content of TiN is 10 vol.%.

Fig. 5 shows the current of TiN-Al_2O_3 ceramic with 5 vol.% TiN under the high voltage. It can be seen that the current of TiN-Al_2O_3 ceramics is very low under the high voltage. The current only 89 nA when the on-load voltage up to 5000V. The ceramics have excellent withstanding ability to the high on-load voltage.

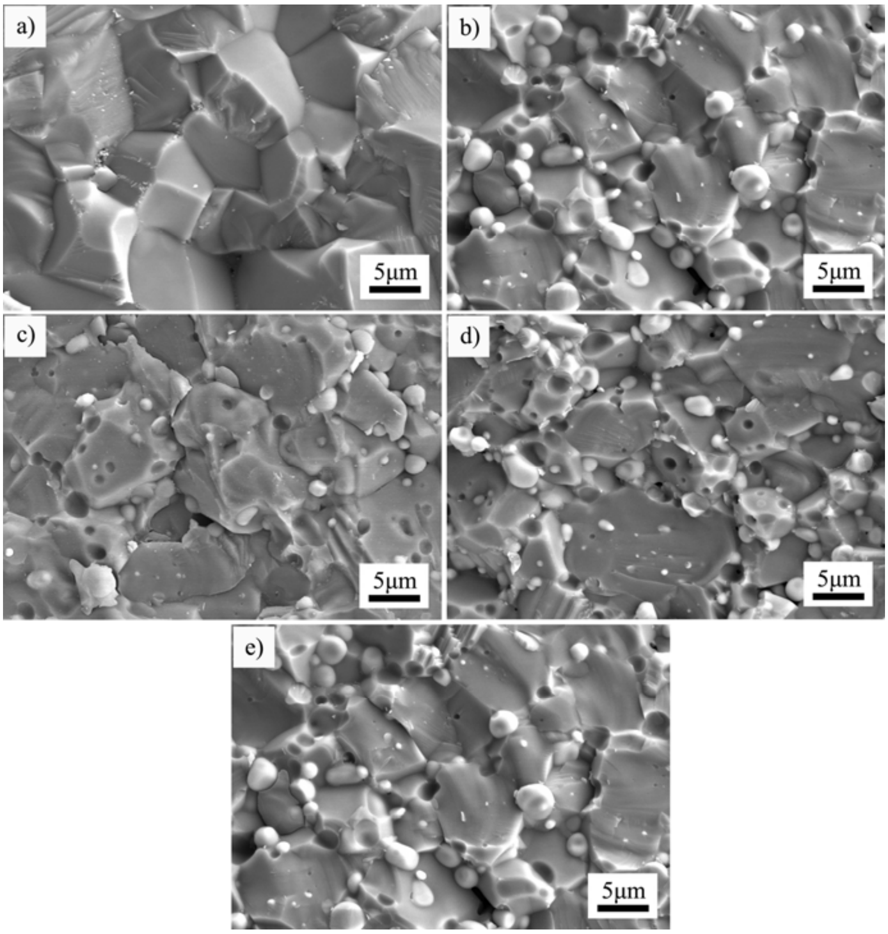

Figure 4. SEM micrograph of fracture cross-sections of the hot-pressed TiN-Al_2O_3 ceramics with different content of TiN. a) 0%, b) 5%, c) 10%, d) 15%, e) 20%

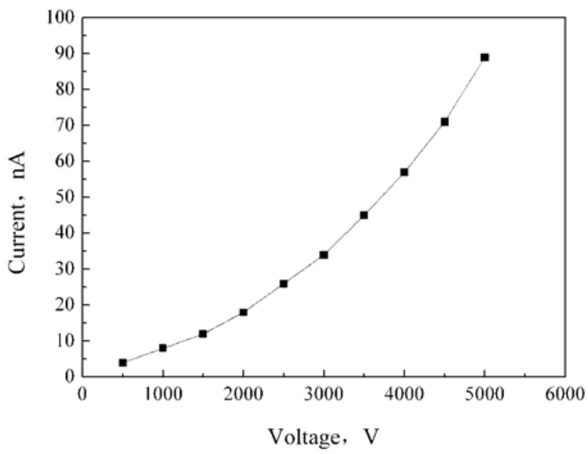

Figure 5. Current of TiN-Al_2O_3 ceramic with 5 vol.% TiN under the high voltage

4. Conclusion

Dense TiN-Al_2O_3 ceramics with high flexural strength, high fracture toughness and very low current under high on-load voltage were successfully prepared by hot pressing with SiO_2 as sintering additives.

The flexural strengths and fracture toughness have been greatly improved and the hardness is almost identical to that of Al_2O_3 matrix. The electrical resistivity of TiN-Al_2O_3 ceramics decreased rapidly with the increasing of the TiN content. The experimental results showed that the TiN-Al_2O_3 ceramics have excellent withstanding ability to the high on-load voltage. The highest current only 89 nA under the 5000 V voltage.

Reference

[1] Wang Y., Wang J., Cheng J., Li Y., Yue Q., H. Chen, Lin J. Production and quality control of STAR-TOF MRPC. *Nucl. Instrum. Meth. A*, **613**, pp. 200-206 (2010).

[2] Zou T., Wang X., Shao M., Sun Y., Zhao Y., Tang H., Ming Y., Guo J., Zhang Y., Li C., Chen H., Xu Z., Zeng H. Quality control of MRPC mass production for STAR TOF. *Nucl. Instrum. Meth. A,* **605**, pp. 282-292 (2009).

[3] Bonnera B., Chenb H., Eppleya G., Geurtsa F., Lamas-Valverde J., Li Ch., Llope W. J., Nussbaum T., Platner E. and Roberts J. A single Time-of-Flight tray based on multigap resistive plate chambers for the STAR experiment at RHIC. *Nucl. Instrum. Meth. A*, **508**, pp.181-184 (2003).

[4] Maiti K., Sil A. Relationship between fracture toughness characteristics and morphology of sintered Al_2O_3 ceramic. *Ceram. Inter*., **36**, pp. 2337-2344 (2010).

[5] Martin C., Cales B., Vivier P. and Mathieu P. Electrical discharge machinable ceramic composites. *Mater. Sci. Eng. A*, **109**, pp. 351-356 (1989).

[6] Rak Z. S., Czechowski J. Manufacture and properties of Al_2O_3-TiN particulate composites. *J. Eur. Ceram. Soc.*, **18**, pp. 373-380 (1998).

[7] Li J., Gao L., Guo J. Mechanical properties and electrical conductivity of TiN-Al_2O_3 nanocomposites. *J. Eur. Ceram. Soc*. **23**, pp. 69-74 (2003).

[8] Shen Z., Johnsson M., Nygren M. TiN/Al_2O_3 composites and graded laminates thereof consolidated by spark plasma sintering. *J. Eur. Ceram. Soc.*, **23**, pp. 1061-1068 (2003).

[9] Chatterjee S., Shariff S.M., Padmanabham G., Dutta Majumdar J., Roy Choudhury A. Study on the effect of laser post-treatment on the properties of nanostructured Al_2O_3-TiB_2-TiN based coatings developed by combined SHS and laser surface alloying. *Surf. Coat. Technol*., **205**, pp. 131-138 (2010).